communications biology

A Nature Portfolio journal

Article

https://doi.org/10.1038/s42003-025-07979-z

Hantaan virus infection induces human mucosal-associated invariant T cell pyroptosis through IRE1α pathway

Yusi Zhang[1,9] ✉, He Liu[2,9], Dalu Liu[3,9], Huiyuan Zhang[1], Ying Ma[1], Na Li[4], Chunmei Zhang[1], Manling Xue[1], Fenglan Wang[5], Xiaozhou Jia[5], Hui Zhang[2], Kang Tang[1], Xiaoyue Xu[1,6], Shijia Wang[1,6], Yiwen Wei[1,7], Xiaojing Yang[2,8], Jiajia Zuo[1,6], Lihua Chen[1], Boquan Jin[1] & Yun Zhang[1] ✉

Hantaan virus (HTNV) triggers an epidemic of hemorrhagic fever with renal syndrome (HFRS), which is predominantly prevalent in Asia. Mucosal-associated invariant T (MAIT) cells, categorized as innate-like T lymphocytes, perform crucial functions in the innate host defense mechanism during virus infection. We previously showed that MAIT cells played antiviral roles in vitro. But marked reduction of MAIT cells was present in the peripheral blood of HFRS patients. Till now, the role of MAIT cells in vivo and the mechanisms of HTNV-induced the MAIT cell deficiency have not yet been fully explored. In this study, by combining the clinical samples, MAIT deficiency mice and in vitro infected MAIT cell models, we find that pyroptosis was the main reason of MAIT cell loss in the peripheral blood of HFRS patients. The molecular mechanisms are related to the overload of calcium in the endoplasmic reticulum (ER) of MAIT cells, which subsequently induces inositol-requiring enzyme-1α (IRE1α)-mediated ER-stress and following pyroptosis. ER-stress inhibitor can reverse the pyroptosis of MAIT cells during HTNV infection. In conclusion, this study firstly reveals the underlying molecular mechanisms for the deficiency of MAIT cells during HTNV infection, and suggests a potential way to stabilize the MAIT cells population in HFRS.

Hantaan virus (HTNV) belongs to the genus Orthohantavirus, family Hantaviridae and order Bunyavirales. The genome of HTNV includes three segments: L (large), M (medium), and S (small). Of those, the S segment encodes nucleocapsid protein (NP). HTNV was transmitted by rodents but only caused hemorrhagic fever with renal syndrome (HFRS) in humans. HFRS is mainly endemic in Asia and Europe. Shaanxi province reported over 10 000 cases in the past 10 years, becoming a major endemic area in China[1]. The symptoms of HFRS includes fever, hemorrhage, and acute renal failure and the clinical course of HFRS is defined by five sequential stages: febrile, hypotensive, oliguric, diuretic, and convalescent. We grouped febrile, hypotensive, and oliguric stages as the acute phase and the diuretic and convalescent stages as convalescent phase. At present, there are no specific therapeutics for HFRS patients causing the disease mortality rate up to 15%. Although inactivated vaccines can robust protective immunity against HTNV infection, the long-term efficacy is uncertain, and vaccine coverage is unsatisfactory[2–4]. How to induce and maintain antiviral immune response during HTNV infection should be studied.

T cells are central elements of the antiviral immune response. During HTNV infection, different subsets of T cells play different roles. For the precise treatment, distinct functions of T cells should be studied systemically. Ma et al. believed that HTNV can infect T cells directly. These virus-infected T cells permitted virus transmission. The functions of these virus-infected T cells were harnessed during the process[5,6]. Zhang et al. reported bystander activation of $CD8^+$T cells mediated pathogenesis in HFRS[7]. Besides above, we also reported that $CD8^+$T cells and a novel subset of $CD4^+$T cells proliferated, produced granzyme B (GrB) and controlled

[1]Department of Immunology, School of Basic Medicine, Fourth Military Medical University, Xi'an, 710032, China. [2]Department of Microbiology, School of Basic Medicine, Fourth Military Medical University, Xi'an, 710032, China. [3]Department of Radiation Medicine and Protection, Ministry of Education Key Lab of Hazard Assessment and Control in Special Operational Environment, School of Public Health, Fourth Military Medical University, Xi'an, 710032, China. [4]Department of Transfusion Medicine, Xijing Hospital, Fourth Military Medical University, Xi'an, 710032 Shaanxi, China. [5]Eighth Hospital of Xi'an, Xi'an, 710061, China. [6]Department of Immunology, School of Basic Medical Sciences, Yan'an university, Yan'an, 716000, China. [7]Department of Pathogenic Biology, School of Basic Medical Sciences, Yan'an university, Yan'an, 716000, China. [8]School of Life Sciences, Yan'an university, Yan'an, 716000, China. [9]These authors contributed equally: Yusi Zhang, He Liu, Dalu Liu. ✉e-mail: immuzys@fmmu.edu.cn; immuzy@fmmu.edu.cn

HTNV infection[8–10]. In addition to that, double positive T cells, which were differentiated from $CD8^+$T cells, exerted protective effects during HTNV infection[11]. In our previous study, we performed scRNA-seq using PBMC from HFRS patients and found that opposite to the other subsets of $CD8^+$T cells, $CD8^+$mucosal associated invariant T (MAIT) cells were decreased significantly in HFRS patients[12]. MAIT cells were innate-like T cells with invariant TCR α chain (Vα7.2-Jα33 in human)[13]. We characterized the phenotypes of MAIT cells and found that MAIT cells were activated by IL-18 and differentiated into effector memory cells during HTNV infection. By producing interferon-γ (IFN-γ) and GrB, they protected HTNV infected-endothelial cells from infection in vitro[12]. However, the lower the frequency and counts of $CD8^+$MAIT cells, the more severe the disease had in HFRS patients. Other researches have also claimed the protective role of MAIT cells during infection[14–16]. MAIT cell-deficient mice show enhanced mortality during lethal influenza infection[17]. Thus, it is important to investigate how to maintain the MAIT cell subset.

Besides us, the deficiency of MAIT cells were also reported in other virus infected diseases. The possible mechanisms included cell pyroptosis, cell apoptosis, activation induced-cell death (AICD) and migrating to the tissues instead[18–21]. However, the deep mechanisms on eliciting the cell death remain unknown.

Endoplasmic reticulum (ER) is the central organelle for protein synthesis, processing. ER stress triggers the unfolded protein response to clear unfolded protein and to restore ER homeostasis[22]. However, if the protein load on the ER greatly exceeds its fold capacity, the cell death is triggered. It is reported that coxsackievirus B3-induced cardiomyocyte apoptosis linked with ER stress[23]. Herpes simplex virus infection activates an ER stress-induced cell death[24]. Besides, the factors in regulating the ER stress are worthy of discussion. It is well known that ER plays an essential role in the regulation of calcium (Ca^{2+}) homeostasis. Breaking the ER calcium homeostasis, such as ER Ca^{2+} reducing or overload can cause ER stress[25,26]. Zhao et al. described that ER Ca^{2+} overload activates the IRE1α signaling mediated ER stress[27]. Chen et al. found that pyroptosis of colorectal cancer cells can be triggered through calcium overload and ER Stress[28]. Although multiple research teams including us have reported that virus infection can induce ER stress in immune cells[29–31], whether MAIT cells deficiency in HTNV infection is associated with ER stress is unknown.

In this study, we performed clinical sample studies, MAIT deficiency mice studies combined with in vitro cell culture studies to further confirm the protective role of MAIT cells during HTNV infection and found that pyroptosis was the major contributor to the deficiency of MAIT cells in the HFRS patients. We also uncovered the underlying mechanisms of pyroptosis of MAIT cells related to ER stress caused by ER Ca^{2+} overload. Our findings will extend the knowledge on the role of MAIT cells in HTNV infection and provide potential MAIT cell-based therapeutic approaches for HFRS patients.

Results

MAIT cells played an antiviral role during HTNV infection

Although we have found that the activation phenotypes and the reduced cell counts of MAIT cells from HFRS patients were correlated with the disease severity, the role of MAIT cells in HTNV infection still needs to be clarified deeply. We co-cultured HTNV infected HUVECs with the serial dilution supernatant collecting from interleukin-12 (IL-12) and IL-18 activated-MAIT cells. The NP of HTNV were detected in HUVECs under different conditions. The results indicated that activation of MAIT cells inhibited the expression of NP in HUVECs (Fig. 1A–B).

Besides in vitro study, we subsequently explored the role of MAIT cells during HTNV infection in vivo. We challenged the $MR1^{-/-}$ (MAIT cells deficiency) mice with HTNV, setting the wild type (WT) mice as control. The body temperature and the body weight of these mice were measured every day post HTNV infection. Although the body weight of the $MR1^{-/-}$ mice did not change significantly compared to the WT mice (Supplementary Fig. 1A), the body temperature of the $MR1^{-/-}$ mice were higher than that of the WT mice at the 2nd day post infection (Fig. 1C). Seven days post infection, the mice were sacrificed. The levels of NP were detected in several organs of the mice. The qPCR results showed that compared to the WT mice, the mRNA level of NP in the lungs and kidneys of $MR1^{-/-}$ mice increased significantly (Fig. 1D), with unsignificant changes in spleen, liver, brain, and heart (Supplementary Fig. 1B). The higher protein levels of NP (red) in the lungs, livers and kidneys of $MR1^{-/-}$ mice were further verified by immunofluorescence results (Fig. 1E-F). Notably, the NP were colocalized with the CD31 expression (green) in the kidney. The percentage of NP^+CD31^+cells were higher in $MR1^{-/-}$ mice than in wild type mice in the kidney, indicating that the endothelial cells were the targets of HTNV in the kidney (Fig. 1G). The pathological changes were only detected in the lungs by HE staining (Supplementary Fig. 1C). Combining the results from clinical sample studies before[12], the in vitro and in vivo studies, we believed that the MAIT cells played an antiviral role during HTNV infection.

The cell death genes were enriched in MAIT cells of HFRS patients

In our previous study, we found that the MAIT cells were clearly decreased in the HFRS patients. The conclusion was further proved by tSNE results of scRNA-seq data, which indicated the reduced number of MAIT cells in HFRS patients (Fig. 2A).

We developed an in vitro viral infection model of MAIT cells. The immunofluorescence images and the flow cytometry results illustrated the expression of nucleoprotein (NP) of HTNV in infected MAIT cells, indicating the successful infection process (Supplementary Fig. 2A–C). The in vitro study also proved that the percentage of MAIT cells in PBMCs was decreased post HTNV infection (Fig. 2B-C).

Some studies reported the decrease of MAIT cells during a kind of viruses' infections. Cell death, the shedding of CD161 molecule, and the MAIT cells migration to the tissues were thought to contribute to the loss of MAIT cells[32–34]. We have shown that the proliferation of MAIT cells were not abrogated in HFRS patients with the increasing of Ki-67 marker. The chemokine receptors on MAIT cells, which drive MAIT cells migrating to tissues, did not change in HFRS patients compared to normal controls[12]. We then analyzed the percentage and cell counts of $CD3^+CD8^+V\alpha7.2^+CD161^-$ cell subsets. The results showed that there was no difference among each comparison groups (Supplementary Fig. 3A–C). The loss of MAIT cells was not due to the shedding of CD161 molecule from MAIT cells.

Next, we stained Annexin V and 7AAD on MAIT cells. The results indicated that the percentage of Annexin V^+ MAIT cells was higher in HFRS patients (Supplementary Fig. 3D–E). According to the scRNA-seq results, the heatmap showed that the cell death related genes were enriched in the MAIT cells from HFRS patients (Fig. 3A). Among these genes, *CYLD, FAS, NFKB1, CASP9, AIM2, CASP1, GSDMD*, and *PYCARD* were significantly upregulated in HFRS patients (Fig. 3A). These genes were correlated with NLRP3 pathway. Then, we detected NLRP3 expression in the MAIT cells. As shown in Fig. 3B and 3C, the protein level of NLRP3 was increased in the HFRS patients. NLRP3 was the main component of inflammasome. Previous studies have reported that the activation of inflammasome could induce the $CD4^+$T cell death in the human immunodeficiency virus (HIV) patients[35]. Based on our scRNA-seq data, we then detected the cleaved Caspase 3 level (Supplementary Fig. 3F–G). The histogram results showed that there was no significant difference of cleaved Caspase 3 level in the MAIT cells between HFRS patients and normal people. Besides, in vitro study also proved that HTNV infection did not induce the increase of Caspase 3 (Supplementary Fig. 3H).

The loss of MAIT cells in HFRS patients was due to pyroptosis

Subsequently, we detected the changes of Caspase 1 in the MAIT cells. The histogram results showed that in HFRS patients, the level of FLICA-Caspase 1 increased significantly (Fig. 3D-E). Not only that, the level of FLICA-Caspase 1 was positively correlated with the level of viral load (Fig. 3F). We also performed Western blot to detect the protein levels of pro-caspase 1 and cleaved-caspase 1 in the sorted MAIT cells. The results showed that the

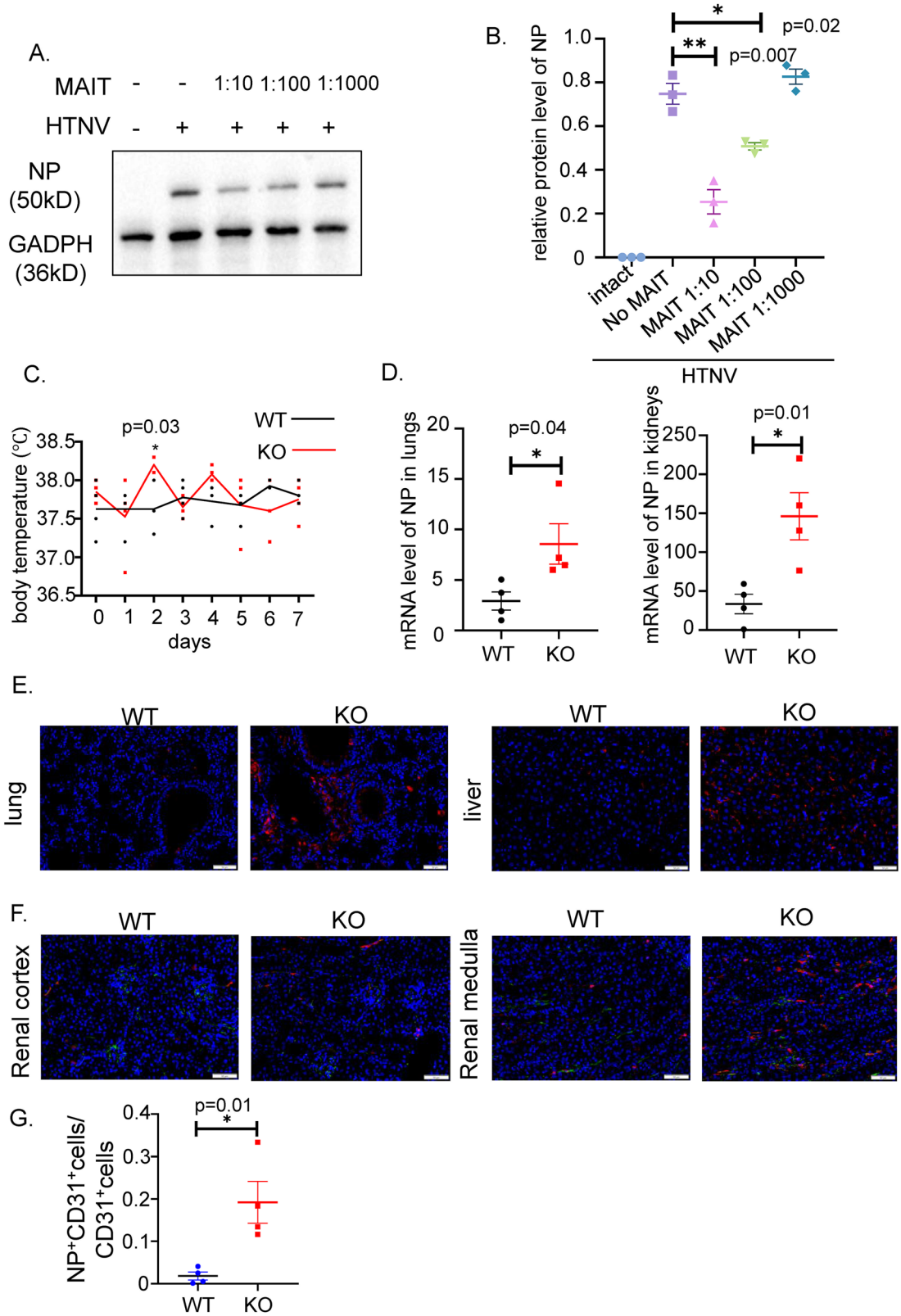

Fig. 1 | The role of MAIT cells in the HTNV infection. A The expression level of nucleotide protein (NP) of HTNV in endothelial cells under different culture conditions. Set untreated HUVEC as a negative control. **B** The statistical analysis of relative NP level corresponding to the GAPDH level ($N = 3$). **C** Body temperature changes were recorded daily in the MAIT deficiency mice ($MR1^{-/-}$) and wild type (WT) mice post HTNV infection. **D** The mRNA level of HTNV NP in the $MR1^{-/-}$ and WT mice 7 days post HTNV infection (NC = 4). **E** The representative immunofluorescence results showed the expression of NP (red) in lungs and livers. Blue: DAPI stained the nucleus. **F** The representative immunofluorescence results showed the co-expression of NP (red) and CD31 (green) in kidney cortex and medulla. Blue: DAPI stained the nucleus. Scale bars, 50 μm. **G** The statistical analysis showing the percentage of NP^+ endothelial cells (CD31) in the kidney. $^*p < 0.05$, $^{**}p < 0.01$.

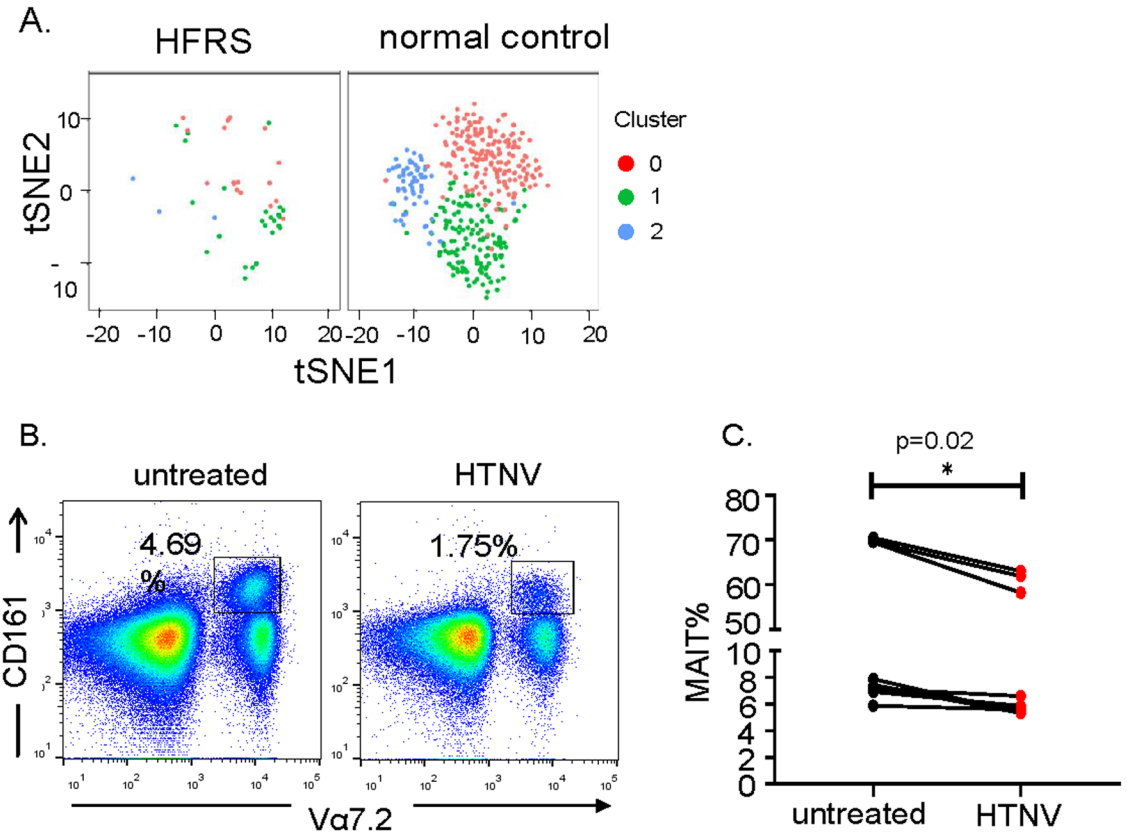

Fig. 2 | HTNV infection caused deficiency of MAIT cells. A t-SNE results showed the cluster 0, 1, and 2 of MAIT cells in HFRS patients and normal controls. **B** Representative flow cytometric graphs and (**C**) cumulative results showing the percentages of MAIT cells during HTNV infection in vitro ($N = 9$). *$p < 0.05$.

MAIT cells from HFRS patients had higher levels of pro-caspase 1 and cleaved-caspase 1 protein levels (Fig. 3G–H).

To further confirm that the pyroptosis was occurred in MAIT cells, we stained the cleaved N terminal gasdermin D protein on the sorted MAIT cells. The staining of HLA-I molecule represented the cell membrane of the MAIT cells. The immunofluorescence results performed by confocol showed that the cleaved N-gasdermin D was expressed on the membrane of MAIT cells from HFRS patients (Fig. 4A). We counted nine views on each slide and calculated the percentage of cleaved N-gasdermin D^+ MAIT cells. The statistic results showed that almost 80% of the MAIT cells from HFRS patients expressed cleaved N-gasdermin D on their membranes (Fig. 4B). We followed up with an imageStream flow cytometry to see the membrane integrity of MAIT cells. Almost 90% MAIT cells in HFRS patients were misshaped (Fig. 4C–D).

We then constructed in vitro HTNV infected MAIT cells model and found that HTNV infection caused FLICA-Caspase 1 increase in MAIT cells compared to untreated MAIT cells (Fig. 5A–B). The immunofluorescence results performed by confocol showed that over 80% MAIT infected with HTNV expressed the cleaved N-gasdermin D on their membranes (Fig. 5C–D). We also detected the protein levels of IL-β and IL-18 in the supernatant of MAIT cells infected by HTNV. The results showed that HTNV infection induced IL-1β and IL-18 production from MAIT cells (Fig. 5E). Based on above, we concluded that HTNV infection induced pyroptosis of MAIT cells, which was the main reason for the reduction of MAIT cells.

IRE1α pathway inhibitor can reverse the pyroptosis of MAIT cells

Next, the reasons of MAIT cells' pyroptosis were explored. The scRNA-seq results presented by violin plots showed that endoplasmic reticulum (ER) stress related genes, including *GRP78, IRE1α*, and *XBP1* were enriched in each cluster of MAIT cells from HFRS patients (Supplementary Fig. 4A). Previous reports demonstrated that GRP78 is a sensor and effector for ER stress, acting as a marker of ER stress. There are three canonical pathways of ER stress, namely IRE1α-sXBP1, PERK-eIF2α-ATF4[36], and the ATF6 pathways. Since the *ATF6* and *PERK* genes were not expressed in each cluster of MAIT cells (Supplementary Fig. 4A), we focused our study on IRE1α pathway. Immunofluorescence images further confirmed that IRE1α molecule was higher expressed in ER (accumulated with KDEL protein) of MAIT cells sorted from HFRS patients (Fig. 6A–B). It was reported that the spliced XBP1 protein (XBP1s) is an activated form of XBP1[37,38]. We examined mRNA level of *XBP1s* by qPCR. The results showed that in vitro infection of HTNV elevated the mRNA level of *XBP1s* (Supplementary Fig. 4B). The above results indicated that HTNV infection induced ER stress and activated IRE1α pathway in MAIT cells.

Although several reports have proved that ER stress stimulated pyroptosis, we still confirmed the role of IRE1α pathway in pyroptosis of MAIT cells during HTNV infection. Firstly, we treated PBMCs with Thapsigargin (TG) (an ER stress inducer) for 24 h, setting untreated PBMCs as controls. The results suggested that although TG treatment only caused slightly decrease of MAIT cells counts (Supplementary Fig. 4C), the level of FLICA-Caspase 1 in MAIT cells were increased under TG treatment (Supplementary Fig. 4D). In vitro infection model results indicated that 4μ8C, the inhibitor of IRE1α pathway, can reverse the effects of pyroptosis caused by HTNV infection. As shown in Fig. 6C–F, compared to HTNV infection alone group, MAIT cells treated with 4μ8C simultaneously with HTNV have increased cell proportion, cell counts and decreased level of FLICA-Caspase 1.

TMCO-1 deficiency was the reason of ER Ca^{2+} overload of MAIT cells

We then asked how did HTNV infection cause ER stress in $CD8^+$ MAIT cells. ER is the main organelle for intracellular Ca^{2+} storage and maintaining intracellular Ca^{2+} homeostasis. Previous studies pointed that ER Ca^{2+} overload could cause ER stress[39], which induced cell pyroptosis

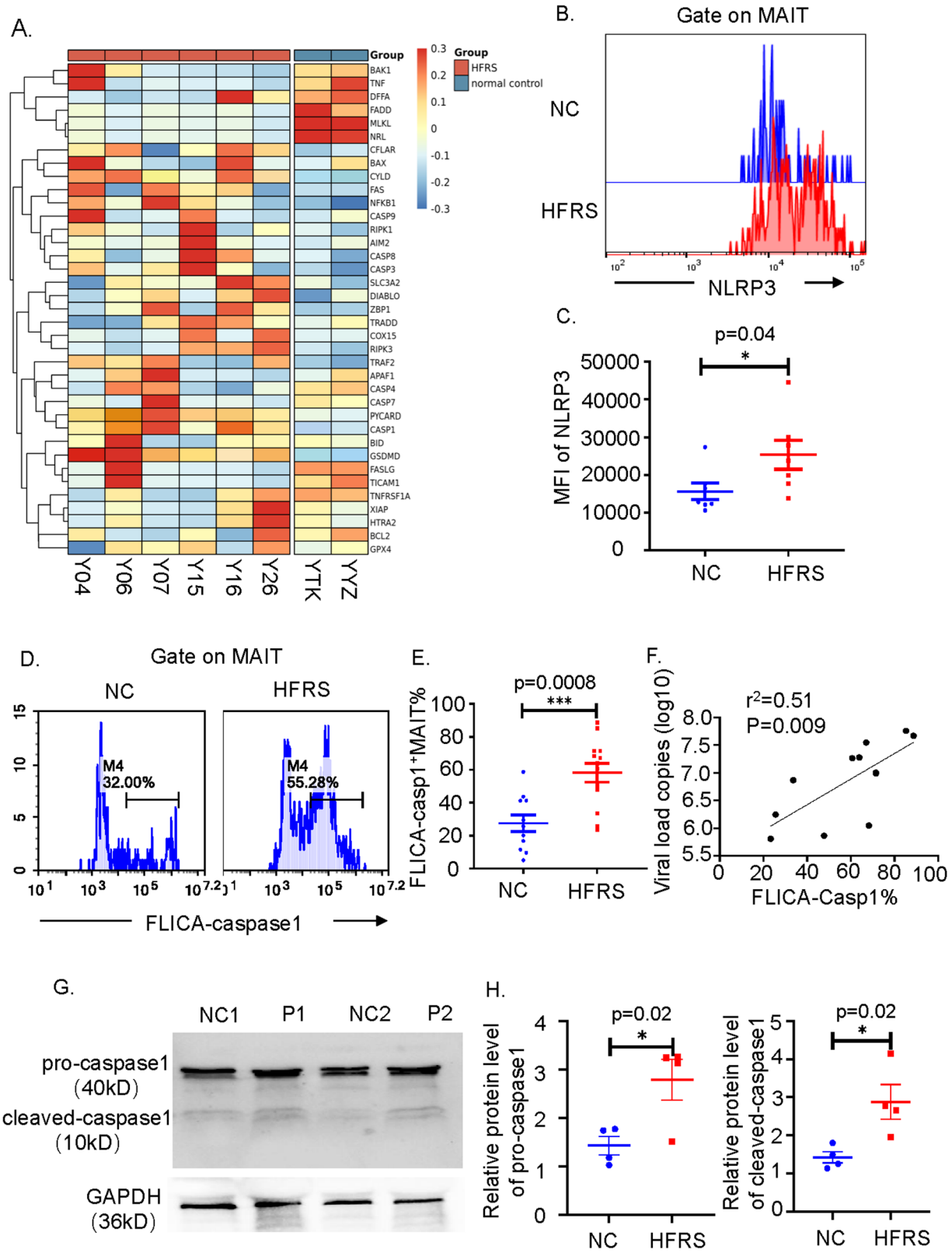

Fig. 3 | The Caspase 1-mediated cell death was the main reason of the MAIT cells reduction in HFRS patients. **A** The heatmap results of scRNA-seq showed the expression profile of cell death genes in MAIT cells from HFRS samples and normal controls. **B** Representative flow cytometric histogram graphs and (**C**) cumulative results showed the expression of NLRP3 in MAIT cells from HFRS samples and normal controls ($N = 7$). **D** Representative flow cytometric histogram graphs and (**E**) cumulative results showed the percentage of FLICA-caspase-1^{+}MAIT cells in HFRS patients and normal controls (HFRS $N = 11$, NC $N = 13$). **F** Correlation between HTNV viral load and proportion of FLICA-caspase-1^{+}MAIT cells. The Pearson correlation coefficient r value and respective p value are shown on the figure. **G**, **H** Western blot results showed the expression levels of the pro-caspase 1 (p40) and cleaved-caspase 1 (p10) in MAIT cells from normal controls (NC) and HFRS patients (P) ($N = 4$). $^{*}p < 0.05$, $^{***}p < 0.001$.

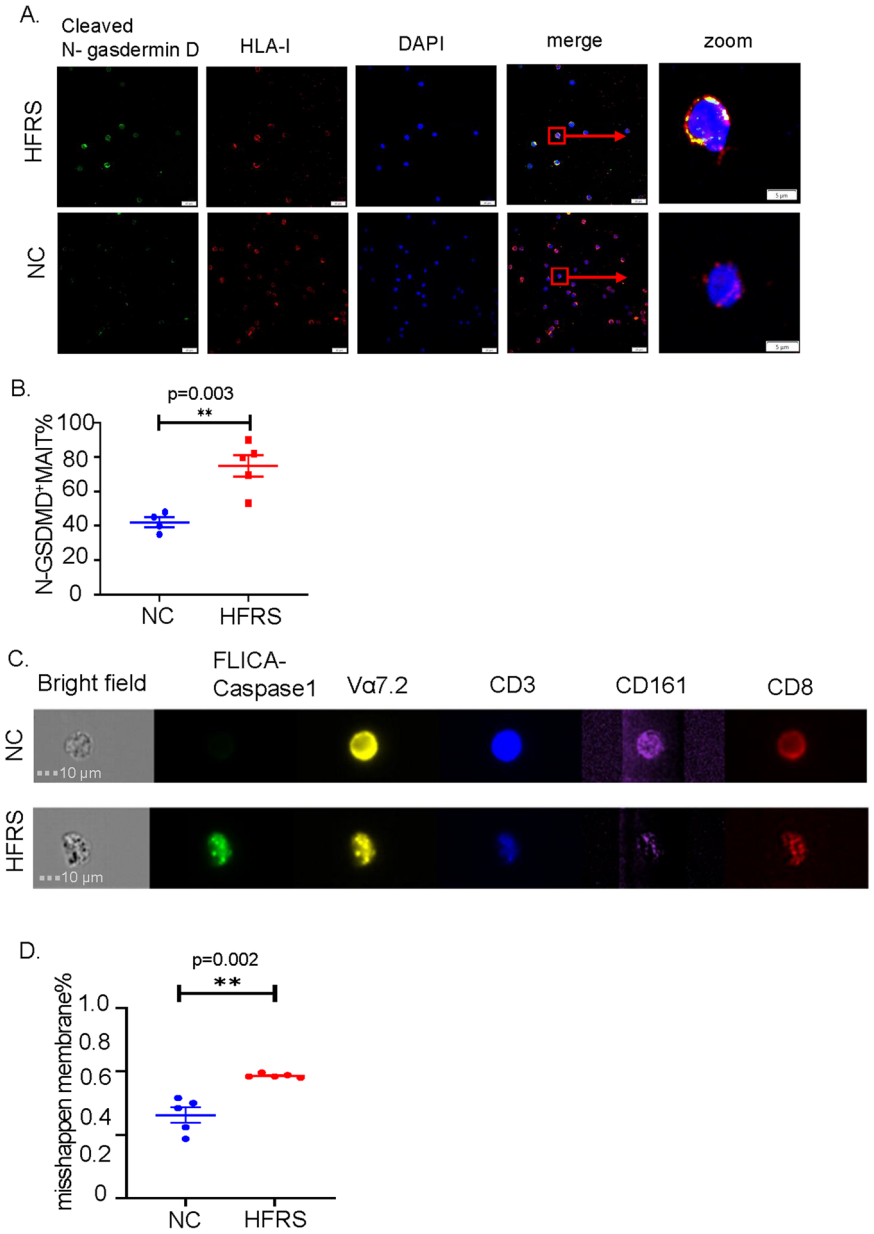

Fig. 4 | Increased pyroptosis in MAIT cells was shown in HFRS patients. A Representative confocol immunoflurescent images and (**B**) quantification of pyroptotic MAIT cells showed the expression of cleaved N terminal Gasdermin D (green) in MAIT cells of HFRS patients and normal controls ($N = 5$). HLA-I staining indicated the cell membrane (red). DAPI staining identifies nucleus (blue). Merge images showed the co-expression of cleaved N terminal-gasdermin D with the cell membrane. Scale bar=20 μm, zoom scale bar=5 μm. **C** Representative image of ImageStream flow cytometric analysis showed MAIT cells from different samples. MAIT cells were stained with FLICA-caspase-1 (green), Vα7.2 (yellow), CD3 (blue), CD161 (purple), and CD8 (red) ($N = 5$). **D** Statistical analysis showed the percentage of cells with misshapen membrane. $^{*}p < 0.05$, $^{**}p < 0.01$.

subsequently[40,41]. Several ER transmembrane proteins, such as TMCO1, VMP1, IP3R, ORAI, and etc, are essential for maintaining ER Ca^{2+} homeostasis[42–45]. The deficiency of these ER Ca^{2+} channel proteins might be one of the factors that would lead to ER Ca^{2+} overload and ER stress.

We performed scRNA-seq to screen these ER Ca^{2+} channels in MAIT cells. By removing the genes that are not expressed in MAIT cells, such as *TRPCs*, the heatmap showed that *TMCO1* was significantly reduced in severe type of HFRS patients in comparison with that in the mild type of HFRS patients and normal controls (Fig. 7A). We then performed flow cytometry using samples from severe HFRS patients in the acute phase. The results proved that corresponding to each isotype control, the TMCO1 was decreased in the severe HFRS patients (Fig. 7B–C). According to the previous studies, we used the ionomycin to measure ER Ca^{2+} stored in MAIT cells. When extracellular Ca^{2+} is chelated with 5 mM EGTA, the rise of cytosolic Ca^{2+} upon ionomycin treatment indicated the intracellular Ca^{2+} mainly released from ER[43,46]. The intracellular Ca^{2+} was monitored using Fluo3/Fura red using Flow cytometry–based measurement. The results showed that ER Ca^{2+} was increased in MAIT cells from HFRS patients (Fig. 7D). These data suggested that TMCO1 deficiency might increase the ER Ca^{2+} store in MAIT cells of HFRS patients. This could be related to the consequences of ER stress and pyroptosis of MAIT cells caused by HTNV infection.

Discussion

In summary, our data found that MAIT cells played a protective role during HTNV infection and uncovered the molecular mechanisms of deficiency of MAIT cells in HFRS patients.

The role of MAIT cells played during infection were debated. Although most of studies stated that MAIT cells exerted an anti-infection effect[17,47], Emgård J et al. found that MAIT cell caused cytokine storm in group A streptococcal toxic shock syndrome[48]. Most of these studies draw conclusions from correlations between the phenotypes of MAIT cells and the severity of the disease. In addition to clinical samples[12], we studied further in this study by challenging $MR1^{-/-}$ mice with HTNV. Our results confirmed the protective role of MAIT cells during HTNV infection. We thought that different subsets of MAIT cells may contribute to the different roles they played in various diseases. MAIT17[49], MAITreg[50], MAIT1[51] cells have been found in succession. Combined with our previous study that MAIT cells

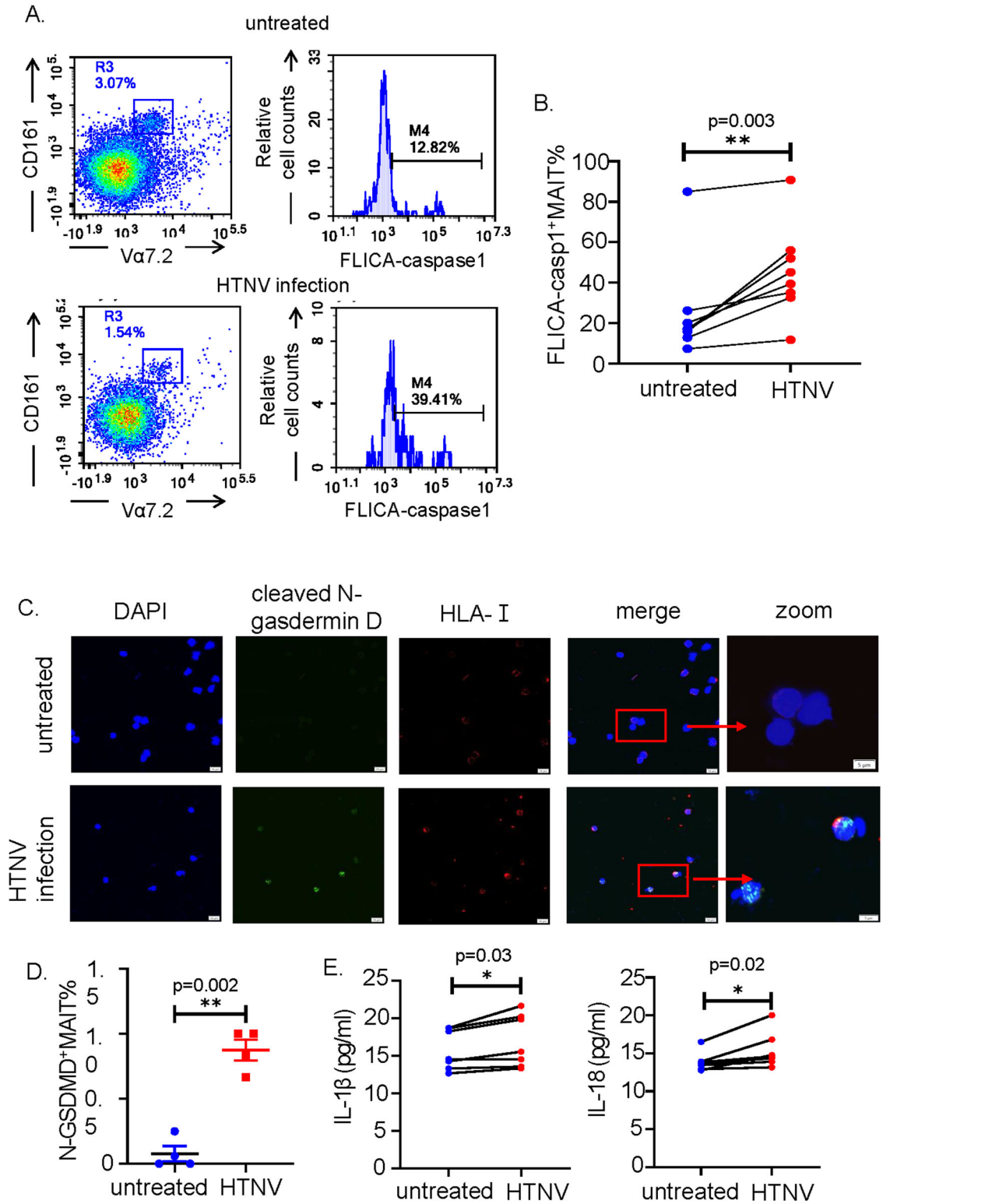

Fig. 5 | In vitro HTNV infection induced pyroptosis of MAIT cells. **A** Representative flow cytometric graphs and (**B**) cumulative results showed the comparison of the percentage of FLICA-caspase-1^{+}MAIT cells in CD3^{+}CD8^{+}T cells post HTNV infection in vitro ($N = 8$). **C** Representative confocol immunoflurescent images and (**D**) quantification of pyroptotic MAIT cells showed cleaved N-terminal gasdermin-D (green) expression in MAIT cells of HFRS patients and normal controls ($N = 5$). HLA-I staining indicated the cell membrane (red). DAPI staining identifies nucleus (blue). Merge images showed the co-expression of cleaved N terminal-gasdermin D with the cell membrane. Scale bar=10 μm, zoom scale bar=5 μm. **E** The level of IL-1β and IL-18 in the supernatant of sorted MAIT cells post HTNV infection in vitro ($N = 7$). $^{*}p < 0.05$, $^{**}p < 0.01$.

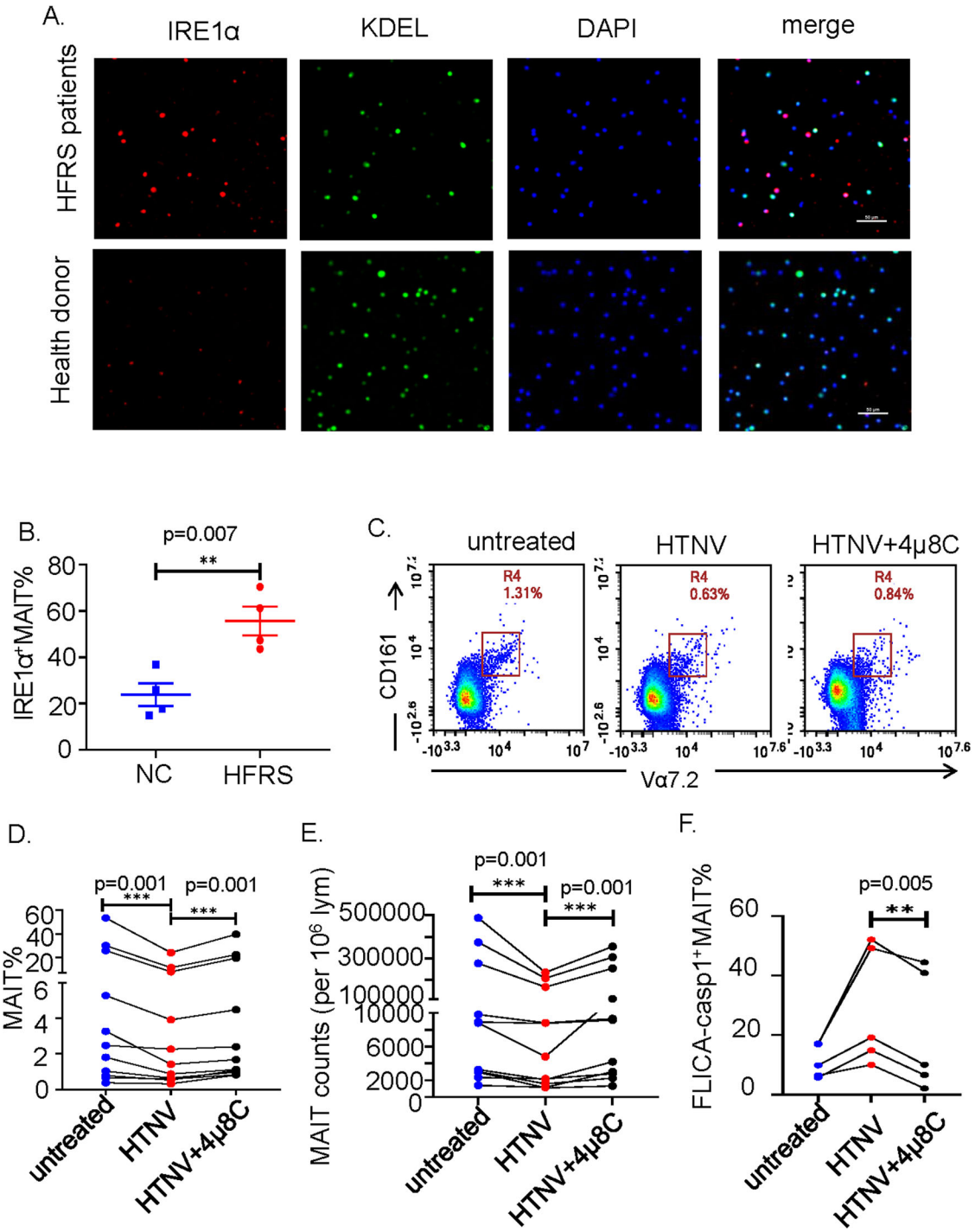

Fig. 6 | IRE1α-mediated ER stress caused pyroptsis of MAIT cells during HTNV infection. A Representative confocol immunoflurescent images and (**B**) quantification of pyroptotic MAIT cells showed the expression of IRE1α (red) in MAIT cells of HFRS patients and normal controls ($N = 4$). KDEL staining indicated the endoplasmic reticulum (ER, green). DAPI staining identifies nucleus (blue). Merge images showed the co-expression of IRE1α with the ER. Scale bar=50 μm. **C** Representative flow cytometric graphs showed the effects of 4μ8C (the inhibitor of IRE1α pathway) on the changes of MAIT cell subset under different treatments. **D** The cumulative statistical results showed the comparison of the percentage and (**E**) cell counts of MAIT cells in different treatment groups ($N = 11$). **F** The cumulative statistical results showed the comparison of the percentage of FLICA-caspase-1$^+$MAIT cells in different treatment groups ($N = 5$). $^*p < 0.05$, $^{**}p < 0.01$, $^{***}p < 0.001$.

predominantly produced IFN-γ and GrB[12], we thought that MAIT cells differentiated to MAIT1 in HTNV infection. Further studies on how HTNV drives MAIT cells differentiation are needed.

Previous findings on HIV infection and Pummala virus (PUUV) infection have shown that the loss of MAIT cells was due to their homing from peripheral blood to tissues[32,33]. In our study, we found that *CCR5*, *CCR6*, and *CCR7* mRNA levels in MAIT cells did not change significantly in HFRS patients compared to the normal controls according to the scRNA-seq data (GSE161354). Other studies on measles virus infection, liver diseases and cardiometabolic diseases assumed that the decrease of MAIT cells was caused by apoptosis[19,52,53]. Consistent with similar studies on COVID-19 patients and chronic HIV infected patients, we also found

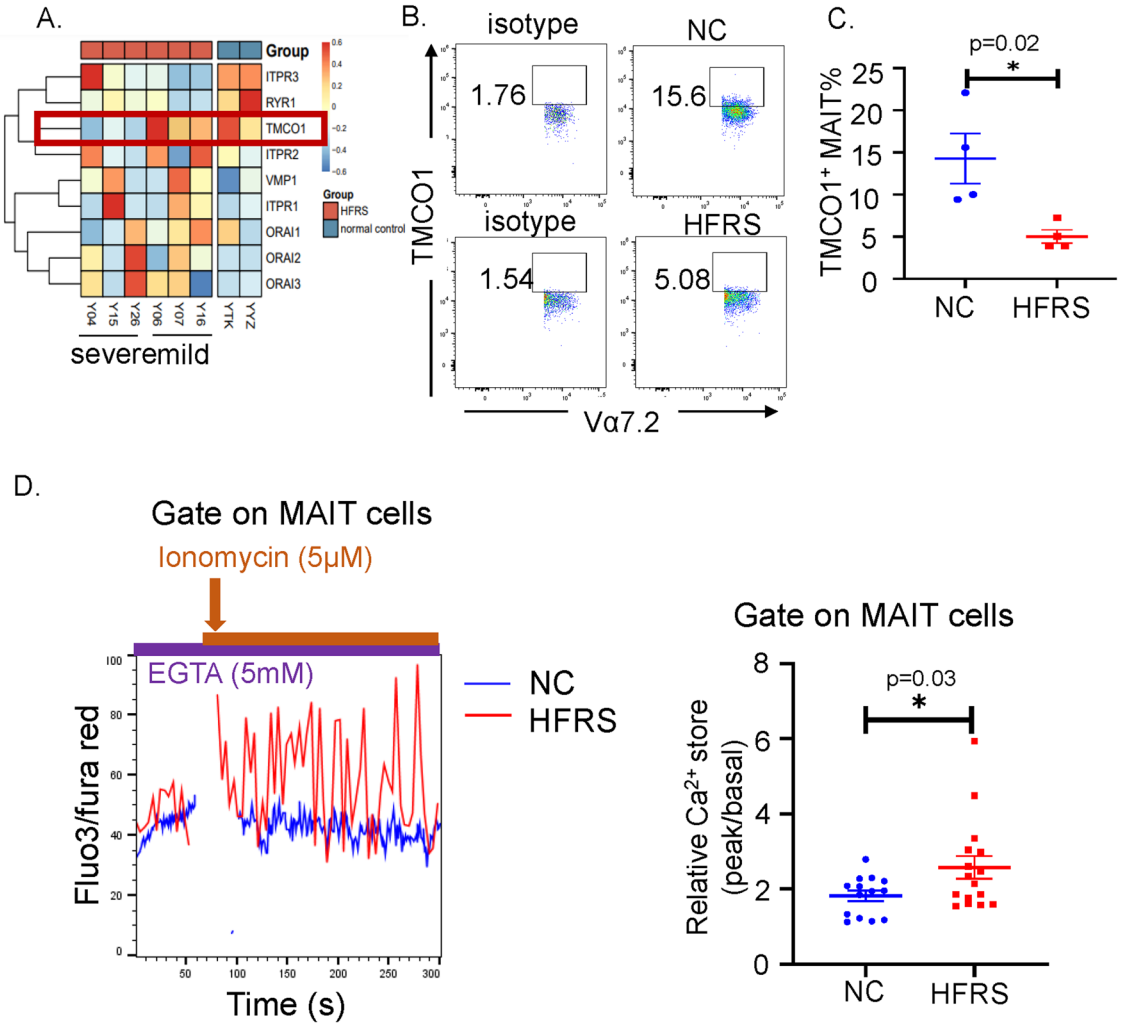

Fig. 7 | TMCO1 deficiency results in ER Ca^{2+} overload. A The heatmap results of scRNA-seq showed the gene expression profile of Ca^{2+} channels on ER. The red rectangle labeled TMCO1 expression in each sample. **B** Representative flow cytometric graphs and (**C**) the cumulative statistical results showed the expression of TMCO1 in MAIT cells from HFRS patients in acute phase and normal controls ($N = 4$). Staining of the cells with isotype-matched control antibody (isotype) served as negative control. **D** Representative flow cytometric graphs and the cumulative statistical results showed ER Ca^{2+} stored in MAIT cells from both HFRS patients and NC ($N = 15$). $^{*}p < 0.05$.

that pyroptosis was the one of the leading causes of MAIT cell death[18,20]. We admitted that AICD and apoptosis were also involved in the loss of MAIT cells during HTNV infection, because the level of *Fas, caspase 3, caspase 8*, and *caspase 9* were increased in MAIT cells from HFRS patients (Fig. 3A). The following results of the protein detection proved that caspase 1 mediated pyroptosis was the predominant mode of cell death. The previous studies focused on the pyroptosis phenotypes of MAIT cells but did not explore the underlying mechanisms. During HTNV infection, almost all the immune cells were activated, especially the $CD8^{+}$T cells. But only $CD8^{+}$MAIT cells were decreased in numbers. We believed that the activation induced pyroptosis was only one of the reasons of MAIT cells' decrease. The in-depth analysis revealed that the TMCO1 deficiency might contribute to inducing the ER stress of MAIT cells. In our previous study, we have shown that NKT cells and $CD4^{+}$T cells were also decreased in HFRS patients[12]. Based on scRNA-seq data, the *TMCO1* in NKT cells and $CD4^{+}$T cells were kept unchanged in HFRS patients compared to normal controls (GSE161354). Interestingly, in our in vitro infection model, the mock HTNV, which lost the replication capability, can also cause the increase of FLICA-Caspase 1 in MAIT cells (Supplementary Fig. 2D–E). We thought that the protein accumulation in MAIT cells may also contribute to the death of MAIT cells. Further studies on the induction of ER stress of MAIT cells, the regulation of TMCO1 expression and on the other types of cell death in different subsets of immune cells during HTNV infection should be performed.

In contrast, Zhao et al. held the opposite view to our study[27]. They described that TMCO1 deficiency caused ER Ca^{2+} overload promoted cell survival. We thought the inconsistence was caused by different types of cell death, different cells, and different stimulations. Both of the apoptotic and pyroptotic cells can be stained with Annexin V[54]. They judged the cell death as apoptosis only by staining the $TMCO1^{-/-}$ HEK 293 T cells or HeLa cells with PI/Annexin V. The interconversions between different types of cell death and the existence of mixed types of cell death should be considered. In our study, we detected the phenotypes of MAIT cells at the present moment. It is hard to construct $TMCO1^{-/-}$ MAIT cells in vitro. Besides, we are still lack of knowledge on the mechanisms that induced TMCO1 deficiency during HTNV infection. Future studies will be needed to test the correlation between the level of TMCO1 in MAIT cells and the viral load of HTNV, the role of TMCO1 in other types of cell death of MAIT cells and the mechanisms regulating the expression of TMCO1 in MAIT cells.

However, this study had some limitations. First, the number of MAIT cells is too limited. It is difficult to overexpress or knockout TMCO1 in vitro to study the following phenotypic effects. It is also hard to collect enough cells to study every target protein in our study. Second, we admitted that the mouse model we used in our study was not the ideal model to study

the HFRS disease. However, till now, there is no proper HFRS disease model worldwide. The HTNV infection has been demonstrated to be pantropic infection in human body and in many laboratory animals. The MAIT cells, which are widely distributed in peripheral blood and mucosal tissues, were collected from peripheral blood of patients and healthy donors in our study. So the microphysiological systems or organoids systems were not applied in the HTNV infection. To further confirm our conclusions, we even obtained the huPBMC-C-NKG mouse model, from Cyagen Bioscience (Catalog Number C001329) by injecting human peripheral blood mononuclear cells (PBMC) into NKG mice. After four weeks of reconstitution, the human $CD45^+$cells were over 70% of total $CD45^+$ cells (both human and mice CD45+ cells). However, most of the cells in humanized mice were classical $CD8^+$T cells. The $CD3^+CD8^+V\alpha7.2^+CD161^{++}$ (MAIT) cell subset was failed to be reconstituted in the humanized mice (Supplementary Fig. 5). Besides, the humanized mice were suffering from the graft versus host disease. The health conditions of the humanized mice were too complicated. Up to now, the humanized mice model is also controversial. Besides, the mouse did not get symptoms of HFRS, it is hard to verify the therapeutic effects of the 4μ8C in the mouse model. Last, in our previous study, we have proved that MAIT cells in HFRS patients were $CD8^+$MAIT cells. So we used CD3, CD8, Vα7.2, and CD161 cell surface markers to identify MAIT cells due to the unavailability of MR1 tetramer. Although these markers are enriched in MAIT cells, they cannot present 100% pure MAIT cells. It would be best to study MAIT cells using MR1 tetramer in the context of HTNV infection.

Conclusion

This study described a protective role of MAIT cells during HTNV infection and the mechanisms of the MAIT cells' deficiency in HFRS patients. We found the ER Ca^{2+} overload induced ER stress might be one of the reasons to the pyroptosis of the MAIT cells. Our findings provide a potential way to rescue the MAIT cells during virus infection and provides some insights to the field.

Methods

Sample collection

A total of 74 samples from 64 individuals were enrolled in this study with ages ranging from 14 to 74 (Table 1). Another 52 healthy volunteers were collected from the physical examination population. The patients' samples were recruited at the Xi'an eighth hospital from November 2012-Januarary 2024. Clinical diagnosis of HFRS was confirmed by the detection of HTNV-specific IgM or IgG antibodies. Peripheral blood samples and plasma were collected as previously described[55]. The ethics committees for human experimentation approved all experiments and sample collection that involved human participants in our study. Four clinical types are classified including mild, moderate, severe, and critical according to the diagnostic criteria from the Prevention and Treatment Strategy of HFRS. The viral load was measured using established protocols[56].

All the sample collection procedures were in accordance with the ethical standards of the responsible committee on human experimentation (Xijing Hospital, First Affiliated Hospital of Fourth Military Medical University, Xi'an, China (NO.KY20243512-1, NO.KY20224214, and NO.KY20224212). Informed consent was obtained from the patients or guardians of patients. All the data were analyzed anonymously. All ethical regulations relevant to human research participants were followed.

Mice

The MAIT cells deficiency mice (C57BL/6JCya-$Mr1^{em1}$/Cya mice, $MR1^{-/-}$ mice) were purchased from Cyagen Biosciences (Suzhou) created by CRISPR-assisted gene targeting strategies. Age- and sex- matched littermates were used in the study. Mice were housed in cages with microisolator tops on ventilated or static racks in a specific pathogen-free facility. Ambient temperature was 20 °C, on a 12-h light dark cycle with automatic light control. Animals were randomized for treatments that were blinded to personnel carrying out the injections and physiological function analysis. Appropriate animal sample size was determined using sample size calculator (http://www.lasec.cuhk.edu.hk/sample-size-calculation.html). All animal works were approved by the Institutional Animal Ethics and Use Committee of the Fourth Military Medical University (NO. 20230275). We have complied with all relevant ethical regulations for animal use.

Cell culture

MAIT cells were enriched by using PE-Vα7.2 antibody and anti-PE Nanobeads (Biolegend) from the peripheral blood mononuclear cells (PBMC) isolated from peripheral blood of human. The MAIT cells were cultured in RPMI 1640 conditioned medium containing 10% fetal bovine serum (Hangzhou Sijiqing Company), 1% Penicillin–streptomycin (Corning), 10 U/ml IL-2 and 20 U/ml IL-7. For stimulation, 20 μM 4μ8c (the inhibitor of IRE1α pathway) and 500 nM thapsigargin (the activator of ER stress) were used for 24 h. For activation, 50 ng/ml IL-12 and 50 ng/ml IL-18 were stimulated for 24 h as reported before.

Human umbilical vessel endothelia cells (HUVECs) were collected as previously described and stored in our lab[57]. The HTNV infected-HUVECs were co-cultured with the serially diluted supernatants of activated MAIT cells. Three days after infection, the protein level of the nucleocapsid protein (NP) of HTNV in HUVECs were measured by Western blot.

HTNV infection

For in vitro infection, Hantaan virus 76-118 strain was propagated in Vero E6 cells using standard methods and the titer was determined using plaque assays[58]. The mock HTNV was prepared by irradiating the HTNV with 1.1×10^4 Gy with ^{60}Co as previously reported. $1\sim2\times10^5$ MAIT cells or PBMCs were seeded in 24 well plate and were exposed to HTNV at multiplicity of infection (MOI) of 2 for 2 h, cultured at 37 °C at 5% CO_2 for 24 h. The cells in control group were left unstimulated. Next, cells were washed and then cultured as above described.

For in vivo infection, male mice aged 5 weeks weighed 20 ± 2 g were chosen in each group. They were challenged with intramuscular injection of the HTNV 76-118 strain (1×10^5 pfu/mouse). Seven days post infection, the mice were sacrificed. Tissue samples from six major organs, including cerebrum, heart, liver, spleen, lung and kidney, were harvested for the HTNV NP detection. The organ tissue lesions were also observed using HE staining.

RNA isolation and qPCR

2×10^5 MAIT cells were seeded in 24 well plate and infected with HTNV for 24 h. The RNA was extracted using TRIzol reagent (Invitrogen) and following its protocols. qPCR was performed using the SYBR Green QPCR Master Mix (Takara) on the Roche LightCycler 480 platform. The xBP1s primer sequences were as follows, Forward, 5'-GCAGGTGCAGGCC CAGTTGT-3', Reverse, 5'-TGGGTCCAAGTTGTCCAGAATGC-3'. The results were normalized to the *β-actin* mRNA level.

Western blot

The collected HUVECs were lysed in RIPA buffer. Western blot (WB) was performed using conventional procedures with 1A8 antibody specific to NP of HTNV, which was kindly provided by the Department of Microbiology, Fourth military Medical University[58]. After developing with 1A8 antibody, the membrane was washed, stripped and re-probed for GAPDH. Band intensity was quantified by ImageJ software. The NP level, pro-caspase1 and cleaved-caspase1 were normalized to the corresponding GAPDH level. Uncropped images can be found at the Supplementary Fig 6.

The sorted MAIT cells from HFRS patients or healthy donors were collected and the similar procedures were performed with the Caspase-1 primary antibody.

Single-cell RNA sequencing (scRNA-seq) data processing and analysis

Sequencing was done as previously described[55]. The data can be found at Public Gene Expression Omnibus database (GSE161354). The information

Table 1 | Characteristics of enrolled subjects

	Mild/ moderate	Severe/ critical	NC
Demographic characteristics			
Number	26	38	52
Age (years)	47 (14–74)	41 (18–70)	36 (23–55)
Male (%)	84.6%	76.3%	65.3%
Sample number	34	40	
Acute phase (febrile/hypotensive/ oliguric)	23	25	_
Convalescent phase (diuretic/ convalescent)	11	15	_

NC normal controls.
Values represent medians with the corresponding interquartile range.

of samples collection was concluded before[55]. The MAIT cells cluster was defined and analyzed as previously described[12].

Flow cytometry analysis

For cell surface staining, 1×10^6 PBMCs from HFRS patients and health donors (setting as normal controls) were stained as previously described. Briefly, antibodies cocktails were added to the cell suspension in 100 µl flow cytometry staining buffer. The primary antibodies used in the study were summarized in the Supplementary Table 1. After incubating the cells at 4 °C in the dark for 30 min, the cells were washed once with staining buffer at 4 °C. Next, cells were subjected to flow cytometry in 100 ul staining buffer.

For intracellular staining, 2×10^6 PBMCs from HFRS patients and health donors (setting as normal controls) were stained with surface markers at first place. Next, cells were fixed and permeabilized using an intracellular staining kit (eBioscience). The cells were then incubated with Cleaved Caspase 3 (Cell Signaling Technology), NLRP3 (Cell Signaling Technology) or TMCO1 (Invitrogen) antibodies in permeabilization buffer at 4 °C for 30 min. After incubating with corresponding second antibodies, cells were resuspended in 100 ul staining buffer.

For apoptosis assay, 1×10^6 PBMCs were stained with MAIT surface markers, then Annexin V and 7-AAD staining were performed following the instructions.

For FLICA-caspase 1 staining assay, 1×10^6 PBMCs were incubated with FLICA-Caspase1 (ImmunoChemistry Technologies) for 1 h at 37 °C in RPMI 1640 medium. After washing twice with 1×washing buffer supplied in the kit, the cells were then stained with MAIT cells' surface markers as mentioned above.

For measurement of ER Ca^{2+} stored in MAIT cells, 3×10^6 PBMCs were prewashed with RPMI 1640 medium containing 5 mM EGTA. These calcium-free medium was used for the whole experiment. Then the cells were loaded with 2 µM Fluo3 and Fura Red dye, CD3-PE-Cy7, CD8-APC-Cy7, Vα7.2-PE, and CD-161-efluro450 in the above medium for 30 min at 37 °C. After washing with the above medium, the cells were resuspended in 200 µl RPMI 1640 medium containing 5 mM EGTA. The samples were placed on the cytometer, recorded 1 min to get the baseline intensities. Then we quickly added 3 µM of ionomycin to the tube. Samples were mixed quickly and recorded for another 4 min.

The samples were acquired with ACEA NovoExpress cytometer (Agilent Bio). The obtained data was analyzed using the FlowJo software (TreeStar), with results expressed in term of a percentage value of the positive cells or mean fluorescence intensity (MFI). In some assay, the images were taken on an Amnis ImageStream X mark II imaging flow cytometer.

Immunofluorescence staining assay

For cells, 2×10^5 sorted MAIT cells under different conditions were spined onto poly-lysine slides by Cytospin (Xiangyi Centrifuge Instrument Co., Ltd., China). Then the cells were fixed with 4% paraformaldehyde for 5 min at room temperature (RT). After washing slides with PBS for twice, the cells were permeabilized with 0.5% triton x-100 in PBS for 20 min at RT. After rinsing twice with PBS, the slides were blocked by goat serum (1:20) for 20 min at RT. The slides were incubated with primary antibodies (Supplementary Table 1), which were 1:200 diluted in PBS containing with 2%BSA + 0.1% Triton X-100 (antibody dilution buffer). After incubation the slides at 4 °C overnight, the slides were rinsed with PBS for five times and were incubated with corresponding fluorescent secondary antibodies.

For tissues, immunofluorescent staining was carried out by Lilai biomedicine. 1A8 antibody or CD31 antibody (Lilai provided) was used as primary antibody. CY3 labeled goat anti-mouse antibody or FITC labeled goat anti-rabbit antibody was used as secondary antibodies. The images were collected by confocal microscopy (Olympus or Nikon, Japan).

The positive cells were counted when they colocalized with DAPI and localization proteins (CD31, HLA-I or KDEL).

HE staining assay

4% paraformaldehyde fixed tissue sections were stained with a hematoxyline and eosine (H&E) using standard techniques. The digital microphotographs were taken at a magnification of ×100 using a computer-assisted image analyzing system. The sections were scanned using automatic digital slice scanning system (Science, Shandong, China).

Enzyme-linked immunosorbent assay (ELISA)

The detection of IL-18 (NeoBioscience, EHC127) and IL-1β (NeoBioscience, EHC002b) in the supernatant were performed using ELISA kits. TECAN Infinite 200pro was used to determine the absorbance at 450 nm. The experiment was performed according to the manufacturer's instructions.

Statistics and Reproducibility

All data analyzed were performed using the GraphPad Prism 8 software. For the correlation analysis, nonparametric Spearman's correlation analysis was used. For the comparisons, two-tailed students *t*-test was used for comparison between the two groups. One-way analysis of variance (ANOVA) was used for comparison between three or more groups. Paired *t* test was used when using paired samples. Data are shown as the mean value±standard error of the mean (SEM) based on more than three independent experiments. In all tests, values of $^*p < 0.05$, $^{**}p < 0.01$, and $^{***}p < 0.001$ were considered statistically significant.

Reporting summary

Further information on research design is available in the Nature Portfolio Reporting Summary linked to this article.

Data availability

The authors declare that all data supporting the findings of this study are available within this article and its Supplementary information files. All the data has been deposited in the Figshare (10.6084/m9.figshare.28466678). Single-cell RNAseq gene expression data have been deposited in the Gene Expression Omnibus database (GSE161354).

Received: 11 September 2024; Accepted: 21 March 2025;
Published online: 01 April 2025

References

1. Liang, W. et al. Mapping the epidemic changes and risks of hemorrhagic fever with renal syndrome in Shaanxi Province, China, 2005-2016. *Sci. Rep.* **8**, 749 (2018).
2. Chen, Y. et al. History of incomplete vaccination may associate with occurrence of hemorrhagic fever with renal syndrome with relieved clinical symptoms. *J. Med Virol.* **88**, 1168–72 (2016).

3. Ren, D. et al. The Clinical Characteristics and Outcomes of Hemorrhagic Fever With Renal Syndrome in Pregnancy. *Front Med (Lausanne)* **9**, 839224 (2022).
4. Yi, Y., Park, H. & Jung, J. Effectiveness of inactivated hantavirus vaccine on the disease severity of hemorrhagic fever with renal syndrome. *Kidney Res Clin. Pr.* **37**, 366–372 (2018).
5. Liu, R. et al. HTNV infection of CD8(+) T cells is associated with disease progression in HFRS patients. *Commun. Biol.* **4**, 652 (2021).
6. Ma, R. et al. T-cell immunoglobulin and mucin 1 (TIM-1) mediates infection of Hantaan virus in Jurkat T cells. *Virus Res* **346**, 199394 (2024).
7. Zhang, X. et al. IL-15 induced bystander activation of CD8(+) T cells may mediate endothelium injury through NKG2D in Hantaan virus infection. *Front Cell Infect. Microbiol* **12**, 1084841 (2022).
8. Ma, Y. et al. Hantaan virus infection induces both Th1 and ThGranzyme B+ cell immune responses that associated with viral control and clinical outcome in humans. *PLoS Pathog.* **11**, e1004788 (2015).
9. Ma, Y. et al. HLA-A2 and B35 restricted hantaan virus nucleoprotein CD8+ T-cell epitope-specific immune response correlates with milder disease in hemorrhagic fever with renal syndrome. *PLoS Negl. Trop. Dis.* **7**, e2076 (2013).
10. Ma, Y. et al. Protective CD8(+) T-cell response against Hantaan virus infection induced by immunization with designed linear multi-epitope peptides in HLA-A2.1/K(b) transgenic mice. *Virol. J.* **17**, 146 (2020).
11. Zhang, H. et al. Increased CD4(+)CD8(+) Double Positive T Cells during Hantaan Virus Infection. *Viruses*. **14**, 1–13 (2022).
12. Zhang, Y. et al. HTNV infection induces activation and deficiency of CD8+MAIT cells in HFRS patients. *Clin. Exp. Immunol.* **211**, 1–14 (2023).
13. Le Bourhis, L. et al. Antimicrobial activity of mucosal-associated invariant T cells. *Nat. Immunol.* **11**, 701–8 (2010).
14. van Wilgenburg, B., et al. MAIT cells are activated during human viral infections. *Nat. Commun.* **7**, 11653 (2016).
15. Rudak, P. T., Choi, J. & Haeryfar, S. M. M. MAIT cell-mediated cytotoxicity: Roles in host defense and therapeutic potentials in infectious diseases and cancer. *J. Leukoc. Biol.* **104**, 473–486 (2018).
16. Flament, H. et al. Outcome of SARS-CoV-2 infection is linked to MAIT cell activation and cytotoxicity. *Nat. Immunol.* **22**, 322–335 (2021).
17. van Wilgenburg, B. et al. MAIT cells contribute to protection against lethal influenza infection in vivo. *Nat. Commun.* **9**, (2018). 4706.
18. Xia, P. et al. Activation-induced pyroptosis contributes to the loss of MAIT cells in chronic HIV-1 infected patients. *Mil. Med Res* **9**, 24 (2022).
19. Rudak, P. T., Yao, T., Richardson, C. D. & Haeryfar, S. M. M. Measles Virus Infects and Programs MAIT Cells for Apoptosis. *J. Infect. Dis.* **223**, 667–672 (2021).
20. Shi, J. et al. Single-Cell Transcriptomic Profiling of MAIT Cells in Patients With COVID-19. *Front Immunol.* **12**, 700152 (2021).
21. Zhang, M. et al. Activation-Induced Cell Death of Mucosal-Associated Invariant T Cells Is Amplified by OX40 in Type 2 Diabetic Patients. *J. Immunol.* **203**, 2614–2620 (2019).
22. Sano, R. & Reed, J. C. ER stress-induced cell death mechanisms. *Biochim Biophys. Acta* **1833**, 3460–3470 (2013).
23. Nie, J. et al. Activation of CaMKII via ER-stress mediates coxsackievirus B3-induced cardiomyocyte apoptosis. *Cell Biol. Int* **44**, 488–498 (2020).
24. Ren, F. et al. ER stress induces caspase-2-tBID-GSDME-dependent cell death in neurons lytically infected with herpes simplex virus type 2. *EMBO J.* **42**, e113118 (2023).
25. Krebs, J., Agellon, L. B. & Michalak, M. Ca(2+) homeostasis and endoplasmic reticulum (ER) stress: An integrated view of calcium signaling. *Biochem Biophys. Res Commun.* **460**, 114–21 (2015).
26. Krebs, J., Groenendyk, J. & Michalak, M. Ca2+-signaling, alternative splicing and endoplasmic reticulum stress responses. *Neurochem Res* **36**, 1198–211 (2011).
27. Zhao, S. et al. ER Ca(2+) overload activates the IRE1alpha signaling and promotes cell survival. *Cell Biosci.* **13**, 123 (2023).
28. Chen, Q. et al. Chondroitin sulfate-modified hydroxyapatite for caspase-1 activated induced pyroptosis through Ca Overload/ER Stress/STING/IRF3 pathway in colorectal cancer. *Small* **20**, 1–13 (2024).
29. Li, Z. et al. ER stress-related molecules induced by Hantaan virus infection in differentiated THP-1 cells. *Cell Stress Chaperones* **26**, 41–50 (2021).
30. Bhoola, N. H. & Kramvis, A. Expression of wild-type or G1862T mutant HBe antigen of subgenotype A1 of hepatitis B virus and the unfolded protein response in Huh7 cells. *J. Gen. Virol.* **98**, 1422–1433 (2017).
31. Fan, Y. & He, J. J. HIV-1 Tat Induces Unfolded Protein Response and Endoplasmic Reticulum Stress in Astrocytes and Causes Neurotoxicity through Glial Fibrillary Acidic Protein (GFAP) Activation and Aggregation. *J. Biol. Chem.* **291**, 22819–22829 (2016).
32. Cosgrove, C. et al. Early and nonreversible decrease of CD161++ /MAIT cells in HIV infection. *Blood* **121**, 951–61 (2013).
33. Maleki, K. T. et al. MAIT cell activation is associated with disease severity markers in acute hantavirus infection. *Cell Rep. Med* **2**, 100220 (2021).
34. Leeansyah, E. et al. Activation, exhaustion, and persistent decline of the antimicrobial MR1-restricted MAIT-cell population in chronic HIV-1 infection. *Blood* **121**, 1124–35 (2013).
35. Zhang, C. et al. NLRP3 inflammasome induces CD4+ T cell loss in chronically HIV-1-infected patients, *J. Clin. Investig*. **131**, 1–12 (2021).
36. Hotamisligil, G. S. Endoplasmic reticulum stress and the inflammatory basis of metabolic disease. *Cell* **140**, 900–17 (2010).
37. Lee, K. et al. IRE1-mediated unconventional mRNA splicing and S2P-mediated ATF6 cleavage merge to regulate XBP1 in signaling the unfolded protein response. *Genes Dev.* **16**, 452–66 (2002).
38. Park, S. M., Kang, T. I. & So, J. S. Roles of XBP1s in Transcriptional regulation of target genes. *Biomedicines*. **9**, 1–26 (2021).
39. Xiong, X. et al. Sarco/endoplasmic reticulum Ca(2+) ATPase (SERCA)-mediated ER stress crosstalk with autophagy is involved in tris(2-chloroethyl) phosphate stress-induced cardiac fibrosis. *J. Inorg. Biochem* **236**, 111972 (2022).
40. Gan, X. et al. Discovery of pyroptosis-inducing drugs and antineoplastic activity based on the ROS/ER Stress/Pyroptosis axis. *Curr. Med. Chem*. **31**, 4880–4897 (2024).
41. Hubinont, C. J. et al. Changes in pancreatic B cell function during late pregnancy, early lactation and postlactation. *Gynecol. Obstet. Invest* **25**, 89–95 (1988).
42. Wang, Q. C. et al. TMCO1 Is an ER Ca(2+) Load-Activated Ca(2+) Channel. *Cell* **165**, 1454–1466 (2016).
43. Liu, Y. et al. VMP1 prevents Ca2+ overload in endoplasmic reticulum and maintains naive T cell survival. *J. Exp. Med*. **220**, 1–14 (2023).
44. Filadi, R. & Pizzo, P. ER-mitochondria tethering and Ca(2+) crosstalk: The IP(3)R team takes the field. *Cell Calcium* **84**, 102101 (2019).
45. Prakriya, M. & Lewis, R. S. Store-Operated Calcium Channels. *Physiol. Rev.* **95**, 1383–436 (2015).
46. Bird, G. S., DeHaven, W. I., Smyth, J. T. & Putney, J. W. Jr Methods for studying store-operated calcium entry. *Methods* **46**, 204–12 (2008).
47. Trivedi, S. et al. Mucosal-associated invariant T (MAIT) cells mediate protective host responses in sepsis, *Elife*. **9** (2020).
48. Emgard, J. et al. MAIT Cells Are Major Contributors to the Cytokine Response in Group A Streptococcal Toxic Shock Syndrome. *Proc. Natl Acad. Sci. USA* **116**, 25923–25931 (2019).
49. Lezmi, G. et al. Circulating IL-17-producing mucosal-associated invariant T cells (MAIT) are associated with symptoms in children with asthma. *Clin. Immunol.* **188**, 7–11 (2018).

50. Fu, S. et al. Regulatory mucosa-associated invariant T cells controlled by beta1 adrenergic receptor signaling contribute to hepatocellular carcinoma progression. *Hepatology* **78**, 72–87 (2023).
51. Salou, M. et al. A common transcriptomic program acquired in the thymus defines tissue residency of MAIT and NKT subsets. *J. Exp. Med* **216**, 133–151 (2019).
52. Touch, S., et al. Mucosal-associated invariant T (MAIT) cells are depleted and prone to apoptosis in cardiometabolic disorders, *FASEB J*, fj201800052RR.(2018).
53. Zhang, Y. et al. Persistent deficiency of mucosa-associated invariant T (MAIT) cells during alcohol-related liver disease. *Cell Biosci.* **11**, 148 (2021).
54. Zhang, J. et al. Mitochondrial-Targeted Delivery of Polyphenol-Mediated Antioxidases Complexes against Pyroptosis and Inflammatory Diseases. *Adv. Mater.* **35**, e2208571 (2023).
55. Zhang, J. et al. The Presence of Circulating Nucleated Red Blood Cells Is Associated With Disease Severity in Patients of Hemorrhagic Fever With Renal Syndrome. *Front Med (Lausanne)* **8**, 665410 (2021).
56. Yi, J. et al. Hantaan virus RNA load in patients having hemorrhagic fever with renal syndrome: correlation with disease severity. *J. Infect. Dis.* **207**, 1457–61 (2013).
57. Zhang, Y. et al. Hantaan virus infection induces CXCL10 expression through TLR3, RIG-I, and MDA-5 pathways correlated with the disease severity. *Mediators Inflamm.* **2014**, 697837 (2014).
58. Zhang, H. et al. Single dose recombinant VSV based vaccine elicits robust and durable neutralizing antibody against Hantaan virus. *NPJ Vaccines* **9**, (2024). 28.

Acknowledgements

This study was supported by grants from the National Natural Science Foundation of China (Dalu Liu 32000876, Ying Ma 82341071, Yun Zhang 82272331), the Natural Science Foundation of Shaanxi Province (Yusi Zhang 2023-JC-YB-640, He Liu 2022SF-510). We thank all the volunteers who generously participated in this study.

Author contributions

Data curation, Yusi Zhang, He Liu and Dalu Liu; Formal analysis, Yusi Zhang, He Liu and Dalu Liu; Funding acquisition, Yusi Zhang, He Liu, Dalu Liu, Ying Ma and Yun Zhang; Investigation, Yusi Zhang, Huiyuan Zhang, Ying Ma, Na Li, Chunmei Zhang and Yun Zhang; Methodology, Yusi Zhang, Huiyuan Zhang, Na Li, Manling Xue, Fenglan Wang, Xiaozhou Jia, Hui Zhang, Xiaoyue Xu, Shijia Wang, Yiwen Wei, Jiajia Zuo; Resources, He Liu, Xiaojing Yang, Na Li, Fenglan Wang, Xiaozhou Jia, Boquan Jin; Software, Yusi Zhang, Ying Ma, Chunmei Zhang, Kang Tang, Shijia Wang, and Yun Zhang; Supervision, Lihua Chen, Boquan Jin and Yun Zhang; Validation, Boquan Jin and Yun Zhang; Writing – original draft, Yusi Zhang and He Liu; Writing – review & editing, Yusi Zhang, Dalu Liu, Boquan Jin and Yun Zhang.

Competing interests

The authors declare no competing interests.

Consent to participate

Informed consent was obtained from all individual participants included in the study. Four participants under the age of 18 were included with the written consent from both themselves and their parents. All the data were analyzed anonymously.

Ethics approval

All procedures were in accordance with the ethical standards of the responsible committee on human experimentation (Xijing Hospital, First Affiliated Hospital of Fourth Military Medical University, Xi'an, China, (NO.KY20243512-1, NO.KY20224214 and NO.KY20224212). All animal studies were performed under the approval of Laboratory animal welfare and ethics committee from Fourth Military Medical University (NO. 20230275).

Additional information

Supplementary information The online version contains supplementary material available at https://doi.org/10.1038/s42003-025-07979-z.

Correspondence and requests for materials should be addressed to Yusi Zhang or Yun Zhang.

Peer review information *Communications Biology* thanks the anonymous reviewers for their contribution to the peer review of this work. Primary Handling Editors: Shitao Li and Johannes Stortz. A peer review file is available.